Brief Communications

# Frequency-Selective Exocytosis by Ribbon Synapses of Hair Cells in the Bullfrog's Amphibian Papilla

**Suchit H. Patel, Joshua D. Salvi, Dáibhid Ó Maoiléidigh, and A. J. Hudspeth**
Howard Hughes Medical Institute and Laboratory of Sensory Neuroscience, The Rockefeller University, New York, New York 10065

**The activity of auditory afferent fibers depends strongly on the frequency of stimulation. Although the bullfrog's amphibian papilla lacks the flexible basilar membrane that effects tuning in mammals, its afferents display comparable frequency selectivity. Seeking additional mechanisms of tuning in this organ, we monitored the synaptic output of hair cells by measuring changes in their membrane capacitance during sinusoidal electrical stimulation at various frequencies. Using perforated-patch recordings, we found that individual hair cells displayed frequency selectivity in synaptic exocytosis within the frequency range sensed by the amphibian papilla. Moreover, each cell's tuning varied in accordance with its tonotopic position. Using confocal imaging, we observed a tonotopic gradient in the concentration of proteinaceous $Ca^{2+}$ buffers. A model for synaptic release suggests that this gradient maintains the sharpness of tuning. We conclude that hair cells of the amphibian papilla use synaptic tuning as an additional mechanism for sharpening their frequency selectivity.**

## Introduction

The auditory organs of tetrapod vertebrates employ complex mechanical and neural mechanisms to discriminate acoustic signals at frequencies ranging from <10 Hz to >100 kHz (Peng and Ricci, 2011). Frequency tuning may be represented as the action of sequential filters, each of which successively attenuates the response to sounds differing from the characteristic frequency at which a cell is most sensitive. The rate at which the response declines as a function of frequency specifies the equivalent number of linear, first-order filters necessary to attain a particular sharpness of tuning.

The frequency selectivity of the mammalian cochlea results primarily from the properties of an active traveling wave upon the basilar membrane (von Békésy, 1960). This wave peaks in only a narrow region—and thereby stimulates only a limited set of hair cells—that depends on the frequency of auditory input (Ruggero et al., 2000). Although this mechanism is absent or rudimentary in non-mammalian tetrapods (Gummer et al., 1987; Manley et al., 1988; O'Neill and Bearden, 1995), the frequency selectivity of their afferent neurons is of comparable quality (Crawford and Fettiplace, 1980; Yu et al., 1991; Manley, 2001). Tuning in these animals benefits from mechanical resonance of the receptor organs and of individual hair bundles (Frishkopf and DeRosier, 1983; Holton and Hudspeth, 1983; Aranyosi and Freeman, 2004). Electrical resonance, a phenomenon in which a hair cell's membrane potential oscillates at particular frequencies, also makes a contribution (Fettiplace and Fuchs, 1999). Because these processes represent only second-order filters, however, they cannot explain completely the observed sharpness of tuning found in auditory afferents, which resembles that of a 10th-order system (Yu et al., 1991; Eatock et al., 1993). Additional mechanisms must contribute to the frequency selectivity of non-mammalian auditory organs. Because synaptic release by saccular hair cells peaks at specific frequencies (Rutherford and Roberts, 2006), the release of neurotransmitter by hair cells might provide an additional degree of tuning. We have therefore investigated the frequency responsiveness of synapses in a tonotopically organized auditory organ, the bullfrog's amphibian papilla.

## Materials and Methods

*Electrophysiology.* All procedures were approved by the Institutional Animal Care and Use Committee of The Rockefeller University. Amphibian papillae were dissected from bullfrogs (*Rana catesbeiana*) of either sex and hair cells were exposed (Keen and Hudspeth, 2006). Dissection and recording were performed in solution containing (in mM): 112 $Na^+$, 2 $K^+$, 1.5 $Ca^{2+}$, 119 $Cl^-$, 3 D-glucose, 2 creatine, 1 pyruvate, and 5 HEPES at pH 7.3 and supplemented with 100 $\mu$M amiloride to minimize $Ca^{2+}$ entry through mechanotransduction channels. The preparation was visualized with differential-interference-contrast optics through a 40× objective lens of numerical aperture 0.8. A calibrated eyepiece reticule was used to determine each cell's distance from the caudal end of the sensory epithelium.

Experiments were conducted at room temperature within 2 h of dissection. Recordings were performed in the whole-cell mode with borosilicate recording pipettes coated with nail polish to reduce their transmural capacitance. Filled with 110 mM $Cs^+$, 2 mM $Na^+$, 2.5 mM $Mg^{2+}$, 113 mM $Cl^-$, 2 mM ATP, 1 mM EGTA, and 10 mM HEPES at pH 7.3, pipettes displayed resistances of 3–10 MΩ. For perforated-patch recordings, the back end of each filament-containing electrode was dipped into this solution for 5–10 s to fill the tip before the shaft was filled with the same solution augmented with 500 $\mu$g/ml amphotericin B (Sigma-Aldrich) freshly dissolved in dimethyl sulfoxide. A stable access

Received March 13, 2012; revised July 31, 2012; accepted Aug. 5, 2012.

Author contributions: S.P., J.S., and A.J.H. designed research; S.P. and J.S. performed research; S.P., J.S., and D.Ó M. analyzed data; S.P., J.S., D.Ó M., and A.J.H. wrote the paper.

This research was supported in part by National Institutes of Health Grant GM07739. D.Ó M. is a Research Associate and A.J.H. is an Investigator of the Howard Hughes Medical Institute. We thank J. A. N. Fisher and S. Lagier for helpful advice, B. Fabella for excellent technical assistance, K. Leitch for expert aid with immunohistochemistry and imaging, and the members of our research group for valuable comments on the manuscript.

The authors declare no competing financial interests.

This article is freely available online through the *J Neurosci* Open Choice option.

Correspondence should be addressed to A. J. Hudspeth, Campus box 314, The Rockefeller University, 1230 York Avenue, New York, NY 10065. E-mail: hudspaj@rockefeller.edu.

DOI:10.1523/JNEUROSCI.1246-12.2012

 0270-6474/12/3213433-06$15.00/0

resistance of 7–15 MΩ developed 5–10 min after formation of a tight seal. Although the series resistance was not compensated, we corrected the holding potential for a liquid-junction potential of −4.3 mV. We rejected recordings in which the capacitance was unstable or in which the access resistance and cell capacitance showed clear correlation.

Experiments were controlled and data recorded with programs written in LabVIEW (National Instruments). Stimuli were delivered and recordings made with a voltage-clamp amplifier (Axopatch 200B, Molecular Devices). Using the lock-in technique (Lindau and Neher, 1988), we assayed each hair cell's capacitance with a 1.5 kHz sinusoidal signal 15 mV in amplitude and centered at −80 mV. Synaptic release was triggered by depolarizing the cell to −55 mV or −45 mV and imposing sinusoidal stimuli 5 mV in amplitude for 1 s at the indicated frequencies in random order. To eliminate artifacts resulting from the hyperpolarization-activated current, we sometimes supplemented the extracellular medium with 50 μM ZD7288 (Tocris Bioscience).

*Measurement of buffer gradients.* Amphibian papillae dissected into cold saline solution were fixed for 1 h at room temperature in PBS solution containing 4% formaldehyde and 0.1% Triton X-100. The tissue was labeled and imaged as previously described (Castellano-Muñoz et al., 2010). Polyclonal rabbit antisera against parvalbumin 3 (Heller et al., 2002) and calbindin-D28k (Swant) were used at respective dilutions of 1:10,000 and 1:1000. Secondary labeling was performed with donkey anti-rabbit IgG conjugated to Alexa Fluor 488 (Invitrogen) at a dilution of 1:500. Phalloidin conjugated to Alexa Fluor 568 (Invitrogen) was used to label hair bundles.

*Z*-stacks were acquired at 0.5 μm intervals with a laser-scanning confocal microscope (Fluoview FV1000, Olympus) bearing a 60× objective lens of numerical aperture 1.35. Images were collected from five or six equally spaced segments along the length of the amphibian papilla. In each image, data from 15–19 cells were analyzed with ImageJ (National Institutes of Health). While holding confocal settings constant for each papilla, we measured pixel intensities in the hair-cell cytoplasm immediately basal to nuclei. To ensure that no artifactitious gradient was introduced by differences in tissue density or other variables, we also stained nuclei with 4′,6-diamidino-2-phenylindole, which showed no significant gradient in fluorescence intensity along the papilla.

*Data analysis.* Data are presented as means ± SEMs for 5–25 presentations of stimuli at each frequency. Capacitance data were averaged for 200 ms immediately before and after each stimulus presentation; the difference between these two values was taken as the resulting capacitance change ($\Delta C_M$). These data are shown for individual cells as a function of the frequency of stimulation. Negative capacitance changes, which sometimes occurred and were assumed to reflect the noise inherent in the recordings, were not indexed as zero but were averaged in the total data set for each cell.

One-tailed paired and unpaired Student's *t* tests were used to determine the significance of capacitance data in which one mean value exceeded the others. Fluorescence data were analyzed by one-way ANOVA. Significance was defined as $p < 0.05$.

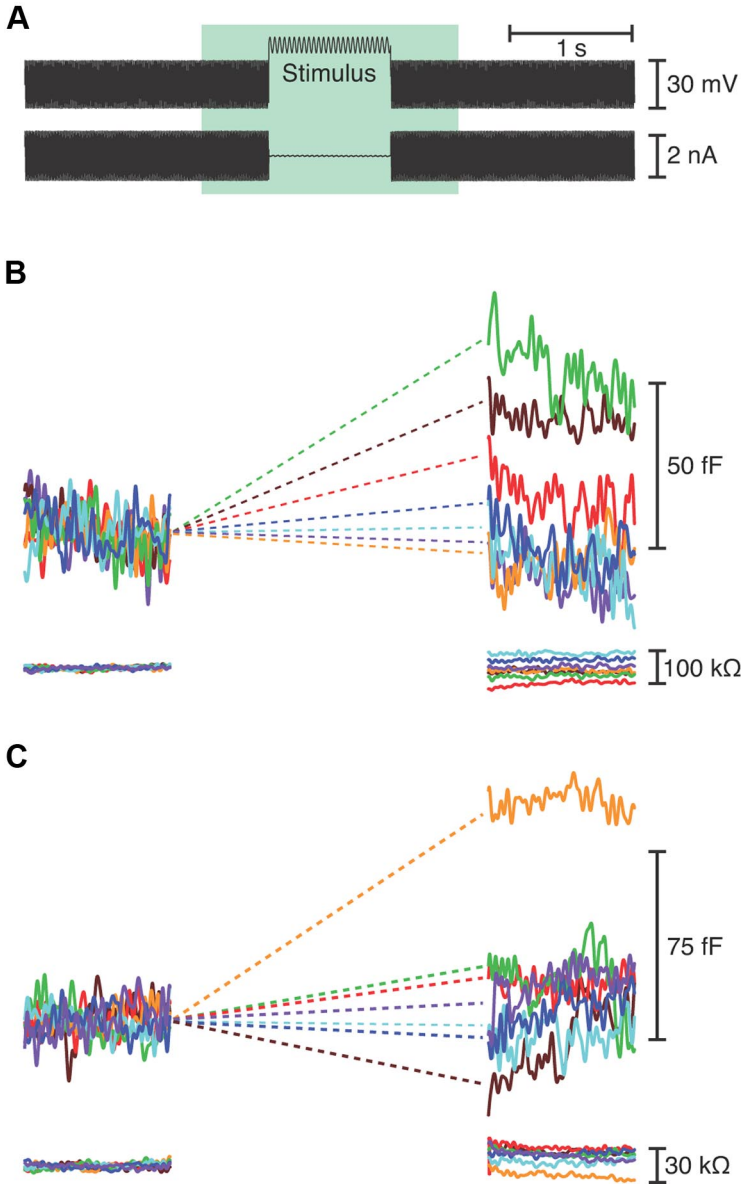


**Figure 1.** Measurement of capacitance changes resulting from exocytosis. ***A***, The upper trace depicts the voltage-clamp protocol used during whole-cell recording in the perforated-patch configuration. A hair cell was held at −80 mV and exposed to a sinuosidal voltage change of ±15 mV at 1500 Hz to measure its membrane capacitance. In the segment labeled Stimulus, the cell was typically depolarized to −55 mV and the capacitance probe was interrupted by a 1 s sinusoidal stimulus at one of seven randomly presented frequencies, usually a constant value, 25, 200, 400, 600, 800, or 1000 Hz. The whole-cell current is shown in the lower trace. ***B***, The upper trace depicts the cell's membrane capacitance, which was averaged over the 200 ms interval immediately before and after stimulation to calculate the capacitance change at the relevant frequency. Increasing frequencies are represented in spectral order. This hair cell, from the mid-frequency region of the papilla, displayed the greatest synaptic exocytosis during stimulation at 400 Hz (green). The lower trace confirms that the access resistance remained stable. ***C***, A rostral cell stimulated at a holding potential of −45 mV showed greatest exocytosis at 300 Hz (orange). Responses to the frequencies used for this cell (100–700 Hz) are shown in spectral order.

*Release-site model.* We simplified the release-site model (Andor-Ardó et al., 2010) by simplifying the parameters, minimizing the level of cooperativity, and reducing the number of states to three: (1) activated, (2) discharged, and (3) loaded. We extended the model by including the dynamics of both $Ca^{2+}$ concentration and of membrane capacitance and by allowing all rate constants to differ. The system is described by

$$\dot{x}_1 = -k_0(1 + \varepsilon x_2^2)x_1 + k_A(1 - x_1 - x_2)C$$

$$\dot{x}_2 = k_0(1 + \varepsilon x_2^2)x_1 - k_R x_2$$

$$\dot{C} = -G(V - E_{Ca}) - k_B BC$$

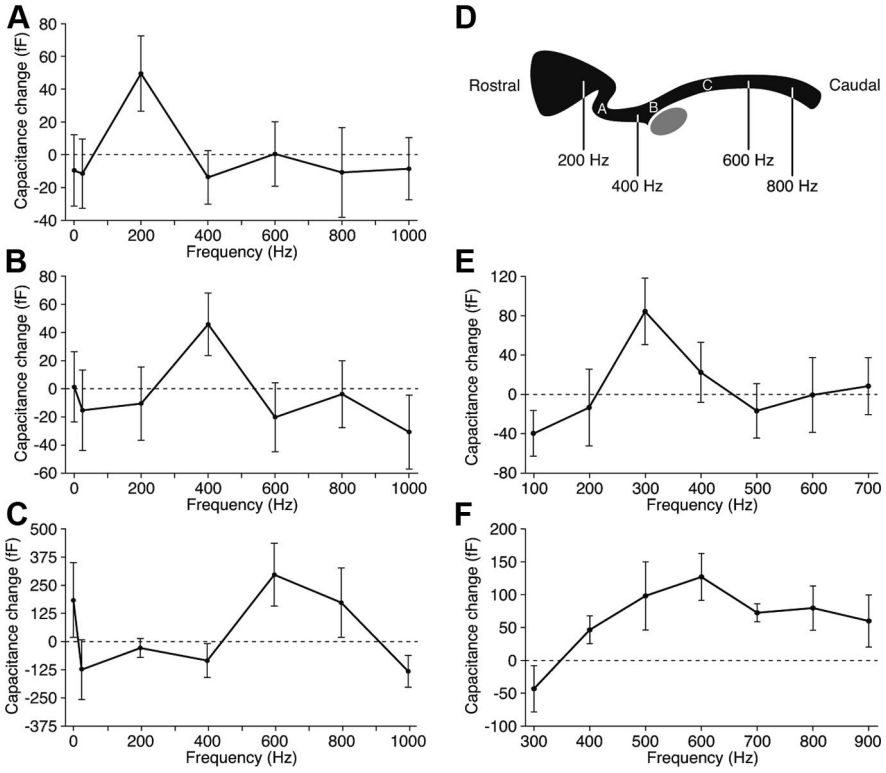


**Figure 2.** Frequency selectivity of exocytosis. ***A***, Synaptic release from a rostrally positioned hair cell peaked for stimulation at 200 Hz. ***B***, A hair cell from the middle portion of the amphibian papilla was most responsive at 400 Hz. ***C***, A cell located nearer the caudal end of the papilla responded best near 600 Hz. In these three and 13 other cells, the capacitance change at the best frequency significantly exceeded that at the flanking frequencies ($p < 0.05$). ***D***, A schematic diagram of the bullfrog's amphibian papilla shows the locations of the three hair cells whose responses are depicted in ***A–C***. The approximate positions of afferent fibers with various characteristic frequencies are indicated (Lewis et al., 1982). The gray ellipse represents the organ's cross-sectioned nerve. ***E***, When held at an elevated potential of −45 mV and stimulated at a more closely spaced set of frequencies, a hair cell from the rostral region of the papilla showed a preferential response to stimulation at 300 Hz. ***F***, A hair cell from the middle portion of the papilla also displayed tuning when stimulated over a narrower range of frequencies.

$$\dot{C}_M = k_0(1 + \varepsilon x_2^2)x_1 N C_V - k_E C_M,$$

in which $x_i$ represents the fraction of sites in state $i$, $k_0$ the vesicle-fusion rate without cooperativity, $\varepsilon$ the cooperativity strength, $k_A$ the rate constant for binding to a release site, $C$ the $Ca^{2+}$ concentration, $k_R$ the rate constant for site recovery, $B$ the buffer concentration, $V$ the membrane potential, $E_{Ca}$ the $Ca^{2+}$ reversal potential, $k_B$ the binding rate constant for $Ca^{2+}$ buffer, $C_M$ the membrane capacitance, $C_V$ the single-vesicle capacitance, $N$ the number of release sites per hair cell, and $k_E$ the rate constant for endocytosis. Top dots represent temporal derivatives. The function

$$G = \frac{g_{MAX}}{2ewN_A(1 + e^{-(V-V_0)/V_S})}$$

accounts for the $Ca^{2+}$ channels' voltage dependence; $g_{MAX}$ is their maximum conductance, $e$ the electron charge, $w$ the hair cell's volume, $N_A$ Avogadro's number, $V_0$ the voltage at which half the channels are open, and $V_S$ their voltage sensitivity.

## Results

### Frequency selectivity of synaptic exocytosis

The amphibian papilla responds to sounds at frequencies from 150 to 1200 Hz (Lewis et al., 1982). To examine the frequency dependence of transmitter release in this organ, we delivered sinusoidal voltage stimuli within this frequency range to individual hair cells voltage-clamped under perforated-patch conditions. We recorded the ensuing changes in membrane capacitance owing to the increase in surface area associated with exocytotic release of neurotransmitter.

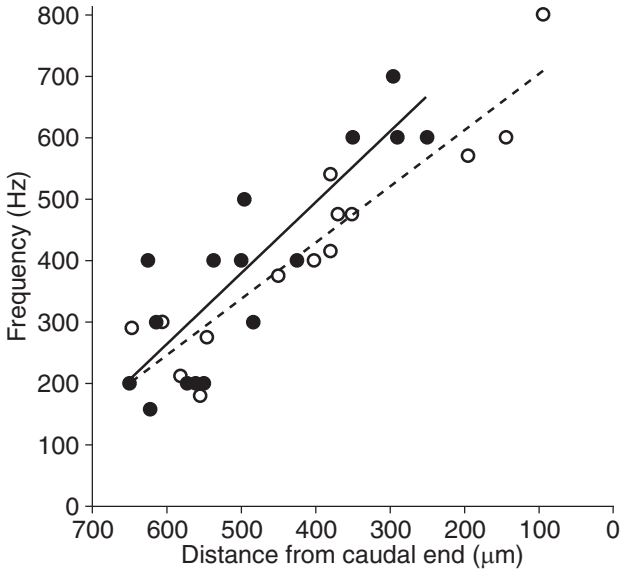


**Figure 3.** Tonotopic organization of synaptic frequency tuning. The frequencies of greatest synaptic release for 16 hair cells (solid circles) are plotted against their distance from the caudal end of the amphibian papilla. The tonotopic map for auditory afferents (Lewis et al., 1982) is shown for comparison (open circles). The coefficients of determination for the linear-regression fits are $R^2 = 0.76$ for the synaptic data and $R^2 = 0.86$ for the afferent responses.

When subjected to 5 mV sinusoidal voltage commands centered at −55 mV, the approximate resting potential, a hair cell responded with a small increase in the total capacitance of its plasmalemma (Fig. 1). We observed in 16 instances a striking preference for a particular stimulation frequency that varied between hair cells. Most cells showed a predilection for frequencies between 200 and 600 Hz, the range of characteristic frequencies for the segment of the sensory epithelium from which we recorded (Fig. 2*A–D*). The increase in the response at a cell's best frequency relative to those at the two flanking frequencies averaged 63 ± 8 fF. Frequency-selective release diminished as each hair cell deteriorated during 10–15 min of recording.

Likely because of the modest synaptic release recorded at a holding potential of −55 mV in our usual recording protocol, we could define only the peaks of tuning curves. To better delineate the sharpness of tuning, we enhanced exocytosis by stimulating hair cells held at a more positive potential of −45 mV. Although deviating somewhat from physiological conditions, this procedure augmented synaptic responses and allowed discrimination of responses at greater frequency resolution. We found that responsiveness declined by more than half as the driving frequency doubled, implying at least first-order low-pass filtering (Fig. 2*E*,*F*). The filtering was even steeper for the high-pass response.

### Spatial distribution of frequency selectivity

To assess possible tonotopic organization, we related the frequency selectivity of synaptic release to the positions of hair cells in the amphibian papilla. The optimal stimulus frequency varied in a systematic way along the sensory epithelium (Fig. 3). Rostral hair cells responded best to stimulation at frequencies as low as 150 Hz, whereas caudal cells exhibited peak responses up to 700 Hz. The best-frequency positions determined by synaptic responsiveness corresponded well with those measured previously from afferent fibers (Lewis et al., 1982).

### Tonotopic variation in the concentration of $Ca^{2+}$ buffers

Because $Ca^{2+}$ buffers influence synaptic function in hair cells (Roberts, 1994), we used immunolabeling to determine which proteinaceous buffers occur in the bullfrog's amphibian papilla. Although only a few hair cells in the rostrolateral region of the papilla expressed calretinin, both parvalbumin 3 and calbindin-D28k occurred widely (Fig. 4*A–F*). We measured the intensity of immunofluorescence in the cytoplasm of individual hair cells along the sensory epithelium and found the labeling of parvalbumin 3 and calbindin-D28k to be, respectively, fourfold and eightfold as strong in high-frequency cells as in low-frequency cells (Fig. 4*C*,*F*). The bullfrog's amphibian papilla thus manifests a tonotopic gradient in $Ca^{2+}$-buffer concentration.

### Model of synaptic tuning

One possible mechanism for synaptic tuning involves cooperative vesicle release (Andor-Ardó et al., 2010). An extension of this model reveals that, for a limited range of buffer concentrations, a regime of spontaneously oscillatory vesicle release is separated from constant release by a loop of Hopf bifurcations (Fig. 4*G*). The zone immediately outside one segment of the loop corresponds to a regime in which synaptic release could be entrained by periodic increases in $Ca^{2+}$ concentration—the signature of synaptic tuning—at frequencies that increase as the buffer concentration rises (Fig. 4*H*). In a real system, the extent of this zone would depend upon the level of noise. The capacitance change in response to sinusoidal voltage changes is large and sharply tuned only when the buffer concentration is chosen such that the system operates near the Hopf bifurcation. Increasing buffer concentration without changing other parameters decreases the resonant frequency (Fig. 4*I*).

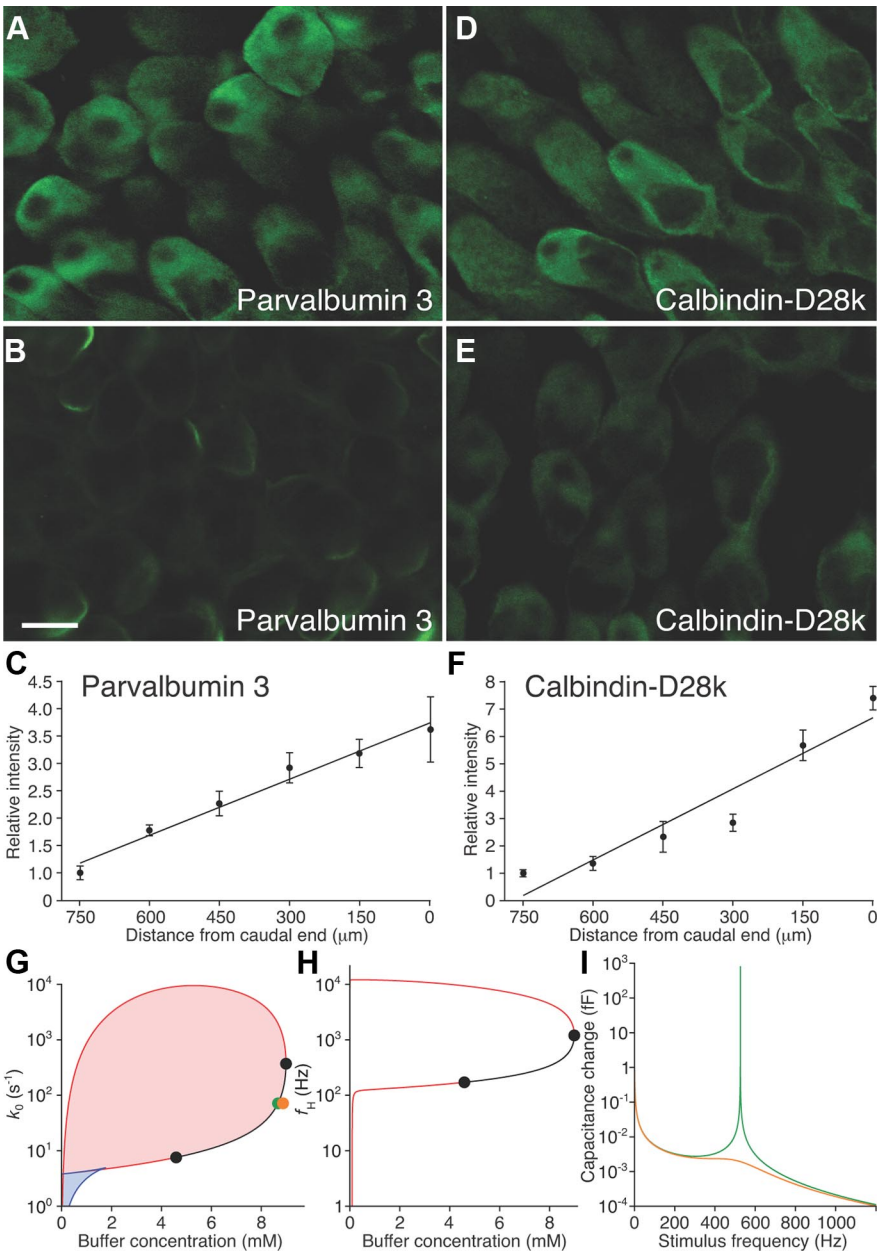


**Figure 4.** Tonotopic distribution of $Ca^{2+}$ buffers. ***A***, Immunofluorescence microscopy detected a relatively high concentration of parvalbumin 3 in hair cells at the caudal, high-frequency end of the amphibian papilla. ***B***, With identical settings of the confocal microscope, hair cells near the rostral, low-frequency end of the organ displayed a lower concentration of parvalbumin 3. ***C***, Parvalbumin 3 labeling increases tonotopically. ***D–F***, Calbindin-D28k occurs at a high concentration in caudal hair cells (***D***) relative to rostral ones (***E***) and displays a tonotopic gradient (***F***). The coefficients of determination for the linear-regression fits are $R^2 = 0.97$ for parvalbumin 3 and $R^2 = 0.91$ for calbindin-D28k. Scale bar: ***A***, ***B***, ***D***, ***E*** (in ***B***), 10 $\mu$m. ***G***, A state diagram describes the release-site model at $-55$ mV as a function of the buffer concentration and the rate constant for vesicle fusion without cooperativity. Spontaneously oscillatory vesicle release occurs in the red shaded region enclosed by a loop of Hopf bifurcations. Two steady states are possible in the blue shaded region demarcated by lines of saddle-node bifurcations (blue). Along the black line, the Hopf bifurcation is supercritical and the Hopf frequency rises as the buffer concentration increases. ***H***, In a plot of the Hopf frequency as a function of the buffer concentration, the resonant frequency equals $f_H$ for points between the black circles at 171 and 1200 Hz. ***I***, The change in capacitance as a function of frequency is much larger and more sharply tuned when the system operates near a Hopf bifurcation (green line; green dot in ***G***) than when the buffer concentration is increased to move the system farther from the bifurcation (orange line; orange dot in ***G***). $E_{Ca} = 90$ mV, $C_V = 34$ aF, $N = 392$, $g_{MAX} = 3.6$ nS, $V_0 = -45$ mV, $V_S = 5$ mV, $w = 6.8$ pl (Graydon et al., 2011), $k_B = 5 \cdot 10^7\ M^{-1} \cdot s^{-1}$ (Schwaller, 2010). $k_E = 0.5\ s^{-1}$ was derived from the decay of the peak capacitance in Figure 1 and agrees with previous measurements (Cho et al., 2011). The parameter values $\varepsilon = 10^8$, $k_A = 7.3 \cdot 10^7\ M^{-1}\ s^{-1}$, and $k_R = 7.6 \cdot 10^4\ s^{-1}$ are constrained by the data presented here.

## Discussion

Individual hair cells of the bullfrog's amphibian papilla release neurotransmitter most effectively during voltage stimulation at frequencies in the range of acoustic stimuli to which the organ best responds. The distribution of best frequencies along the organ accords with the tonotopic map based on afferent-fiber activity (Lewis et al., 1982) and with the pattern of electrical resonance (Smotherman and Narins, 1999). Hair cells of the amphibian papilla therefore display a tonotopic gradient in the efficacy of transmitter release.

What accounts for the difference between the present findings and an earlier investigation that showed no frequency-selective exocytosis in the amphibian papilla of the grass frog (Quiñones et al., 2012)? First, the previous study pooled data from numerous cells in two large segments of the papilla, potentially obscuring sharp tuning curves. Second, the frequency resolution used here exceeded that used in the earlier study and was therefore more likely to have revealed sharp tuning. Finally, the earlier recordings were conducted in the conventional whole-cell recording configuration as opposed to the perforated-patch mode. This difference suggests that soluble proteins, perhaps including $Ca^{2+}$ buffers, are of critical importance for the mechanism of frequency selectivity. Supporting this notion is the papilla's conspicuous gradient of the $Ca^{2+}$-buffering proteins parvalbumin 3 and calbindin-D28k. Our observations accord with those of buffer gradients in other hearing organs (Hiel et al., 2002; Hackney et al., 2003; Schnee et al., 2005), raising the possibility that synaptic tuning occurs elsewhere as well, particularly in non-mammalian systems lacking sharply tuned traveling waves (Gummer et al., 1987; Manley et al., 1988; O'Neill and Bearden, 1995).

The release-site model shows how buffer concentration might influence synaptic tuning. Although tonotopic gradients of additional proteins are likely, the frequency range of the model could be matched to that of the amphibian papilla by systematic variation of only the buffer concentration and the rate constant for vesicle fusion. In this model a rise in the buffer concentration would not increase the resonant frequency but rather ensure that the system operates near a Hopf bifurcation, thereby keeping the system sensitive and sharply tuned. It is a noteworthy prediction of this model that lowering the buffer concentration, for example by whole-cell recording, could bring a hair cell into a regime in which spontaneous release of transmitter by individual synapses becomes rhythmic. This effect might be apparent in recordings of postsynaptic activity.

Because we have assumed no concurrent endocytosis during the 1 s voltage stimuli, the measured capacitance changes are likely underestimates of the actual exocytotic responses. Our results nevertheless imply that tuning can result from interactions involving primarily the readily releasable pool of synaptic vesicles. If each vesicle contributes a capacitance of 34 aF, 1000 vesicles are released by 50 synaptic ribbons during 1 s of stimulation (Graydon et al., 2011). This increment of 20 additional vesicles released per synapse is well within a ribbon synapse's exocytotic capacity of several hundred per second (Parsons et al., 1994). Our experiments are unlikely to have wholly depleted the readily releasable pool of 15 vesicles per active zone (Graydon et al., 2011), which can refill in 15–200 ms (Spassova et al., 2004; Cho et al., 2011). Because natural tones are seldom present for longer than a few tens to hundreds of milliseconds, this pool likely mediates tuned synaptic responses *in vivo*.

The frequency dependence of synaptic release constitutes a bandpass filter. From recordings at closely spaced frequencies in more depolarized cells, we observed low-pass responses that decreased by half as the frequency doubled and high-pass responses that sometimes declined even more rapidly. These results can therefore account for at least two orders of the overall sharpening of auditory-nerve responses. It is possible that synaptic filtering *in vivo* is still sharper, for the accumulation of $Ca^{2+}$ in the presynaptic cytoplasm during prolonged depolarization might saturate synaptic release and thus broaden the tuning. However, given the small synaptic responses to short stimuli near the resting potential, the resolution of capacitance recording did not allow us to precisely delineate tuning at the resting potential.

The afferent fibers of the amphibian papilla display frequency selectivity comparable to that of the auditory organs in other vertebrates including mammals (Yu et al., 1991; Schoffelen et al., 2008). Although electrical resonance contributes to frequency selectivity in the low-frequency region of the papilla (Smotherman and Narins, 1999), it is insufficient to account for the documented sharpness of tuning. The amphibian papilla lacks a flexible basilar membrane that could support traveling waves (Wever, 1973). Although the overlying tectorium might bear traveling waves (Hillery and Narins, 1984), its function in tuning remains hypothetical. Other tuning mechanisms must therefore account for the sharp tuning found in auditory afferents. We propose that the tonotopic tuning of hair-cell synapses plays an important role in sharpening the frequency selectivity of the amphibian papilla.

## References


Andor-Ardó D, Hudspeth AJ, Magnasco MO, Piro O (2010) Modeling the resonant release of synaptic transmitter by hair cells as an example of biological oscillators with cooperative steps. Proc Natl Acad Sci U S A 107:2019–2024. CrossRef Medline

Aranyosi AJ, Freeman DM (2004) Sound-induced motions of individual cochlear hair bundles. Biophys J 87:3536–3546. CrossRef Medline

Castellano-Muñoz M, Israel SH, Hudspeth AJ (2010) Efferent control of the electrical and mechanical properties of hair cells in the bullfrog's sacculus. PLoS One 5:e13777. CrossRef Medline

Cho S, Li GL, von Gersdorff H (2011) Recovery from short-term depression and facilitation Is ultrafast and $Ca^{2+}$ dependent at auditory hair cell synapses. J Neurosci 31:5682–5692. CrossRef Medline

Crawford AC, Fettiplace R (1980) The frequency selectivity of auditory nerve fibres and hair cells in the cochlea of the turtle. J Physiol 306:79–125. Medline

Eatock RA, Saeki M, Hutzler MJ (1993) Electrical resonance of isolated hair cells does not account for acoustic tuning in the free-standing region of the alligator lizard's cochlea. J Neurosci 13:1767–1783. Medline

Fettiplace R, Fuchs PA (1999) Mechanisms of hair cell tuning. Annu Rev Physiol 61:809–834. CrossRef Medline

Frishkopf LS, DeRosier DJ (1983) Mechanical tuning of free-standing stereociliary bundles and frequency analysis in the alligator lizard cochlea. Hear Res 12:393–404. CrossRef Medline

Graydon CW, Cho S, Li GL, Kachar B, von Gersdorff H (2011) Sharp $Ca^{2+}$ nanodomains beneath the ribbon promote highly synchronous multivesicular release at hair cell synapses. J Neurosci 31:16637–16650. CrossRef Medline

Gummer AW, Smolders JW, Klinke R (1987) Basilar membrane motion in the pigeon measured with the Mössbauer technique. Hear Res 29:63–92. CrossRef Medline

Hackney CM, Mahendrasingam S, Jones EM, Fettiplace R (2003) The distribution of calcium buffering proteins in the turtle cochlea. J Neurosci 23:4577–4589. Medline

Heller S, Bell AM, Denis CS, Choe Y, Hudspeth AJ (2002) Parvalbumin 3 is an abundant $Ca^{2+}$ buffer in hair cells. J Assoc Res Otolaryngol 3:488–498. CrossRef Medline

Hiel H, Navaratnam DS, Oberholtzer JC, Fuchs PA (2002) Topological and developmental gradients of calbindin expression in the chick's inner ear. J Assoc Res Otolaryngol 3:1–15. CrossRef Medline

Hillery CM, Narins PM (1984) Neurophysiological evidence for a traveling

wave in the amphibian inner ear. Science 225:1037–1039. CrossRef Medline

Holton T, Hudspeth AJ (1983) A micromechanical contribution to cochlear tuning and tonotopic organization. Science 222:508–510. CrossRef Medline

Keen EC, Hudspeth AJ (2006) Transfer characteristics of the hair cell's afferent synapse. Proc Natl Acad Sci U S A 103:5537–5542. CrossRef Medline

Lewis E, Leverenz E, Koyama H (1982) The tonotopic organization of the bullfrog amphibian papilla, an auditory organ lacking a basilar membrane. J Comp Physiol A Neuroethol Sens Neural Behav Physiol 145:437–445. CrossRef

Lindau M, Neher E (1988) Patch-clamp techniques for time-resolved capacitance measurements in single cells. Pflügers Arch Eur J Physiol 411:137–146. CrossRef

Manley GA (2001) Evidence for an active process and a cochlear amplifier in nonmammals. J Neurophysiol 86:541–549. Medline

Manley GA, Yates GK, Köppl C (1988) Auditory peripheral tuning: evidence for a simple resonance phenomenon in the lizard *Tiliqua.* Hear Res 33:181–189. CrossRef Medline

O'Neill MP, Bearden A (1995) Laser-feedback measurements of turtle basilar membrane motion using direct reflection. Hear Res 84:125–138. CrossRef Medline

Parsons TD, Lenzi D, Almers W, Roberts WM (1994) Calcium-triggered exocytosis and endocytosis in an isolated presynaptic cell: capacitance measurements in saccular hair cells. Neuron 13:875–883. CrossRef Medline

Peng AW, Ricci AJ (2011) Somatic motility and hair bundle mechanics, are both necessary for cochlear amplification? Hear Res 273:102–122. CrossRef Medline

Quiñones PM, Luu C, Schweizer FE, Narins PM (2012) Exocytosis in the frog amphibian papilla. J Assoc Res Otolaryngol 13:39–54. CrossRef Medline

Roberts WM (1994) Localization of calcium signals by a mobile calcium buffer in frog saccular hair cells. J Neurosci 14:3246–3262. Medline

Ruggero MA, Narayan SS, Temchin AN, Recio A (2000) Mechanical bases of frequency tuning and neural excitation at the base of the cochlea: comparison of basilar-membrane vibrations and auditory-nerve-fiber responses in chinchilla. Proc Natl Acad Sci U S A 97:11744–11750. CrossRef Medline

Rutherford MA, Roberts WM (2006) Frequency selectivity of synaptic exocytosis in frog saccular hair cells. Proc Natl Acad Sci U S A 103:2898–2903. CrossRef Medline

Schnee ME, Lawton DM, Furness DN, Benke TA, Ricci AJ (2005) Auditory hair cell-afferent fiber synapses are specialized to operate at their best frequencies. Neuron 47:243–254. CrossRef Medline

Schoffelen RL, Segenhout JM, van Dijk P (2008) Mechanics of the exceptional anuran ear. J Comp Physiol A Neuroethol Sens Neural Behav Physiol 194:417–428. CrossRef Medline

Schwaller B (2010) $Ca^{2+}$ buffers. In: Handbook of cell signaling (Bradshaw RA, Dennis EA, eds), pp 955–962. Amsterdam: Elsevier.

Smotherman MS, Narins PM (1999) The electrical properties of auditory hair cells in the frog amphibian papilla. J Neurosci 19:5275–5292. Medline

Spassova MA, Avissar M, Furman AC, Crumling MA, Saunders JC, Parsons TD (2004) Evidence that rapid vesicle replenishment of the synaptic ribbon mediates recovery from short-term adaptation at the hair cell afferent synapse. J Assoc Res Otolaryngol 5:376–390. CrossRef Medline

von Békésy G (1960) Experiments in hearing. New York: McGraw-Hill.

Wever EG (1973) The ear and hearing in the frog, *Rana pipiens.* J Morphol 141:461–477. CrossRef Medline

Yu XL, Lewis ER, Feld D (1991) Seismic and auditory tuning curves from bullfrog saccular and amphibian papillar axons. J Comp Physiol A Neuroethol Sens Neural Behav Physiol 169:241–248. CrossRef